Available online at www.sciencedirect.com
ScienceDirect
Nuclear Instruments and Methods in Physics Research A 585 (2008) 83–87
NUCLEAR INSTRUMENTS & METHODS IN PHYSICS RESEARCH Section A
www.elsevier.com/locate/nima

Position resolution of a high efficiency transition radiation detector for high counting rate environments

M. Klein-Bösing[a,*], A. Andronic[c], D. Bartoş[b], I. Berceanu[b], V. Cătănescu[b], C. Garabatos[c], N. Heine[a], A. Herghelegiu[b], C. Măgureanu[b], D. Moisă[b], M. Petriş[b], M. Petrovici[b], A. Radu[b], V. Simion[b], F. Uhlig[c], J.P. Wessels[a], A. Wilk[a]

[a]*Institut für Kernphysik, University of Münster, Germany*
[b]*NIPNE Bucharest, Romania*
[c]*GSI Darmstadt, Germany*

Received 16 July 2007; received in revised form 8 October 2007; accepted 5 November 2007
Available online 17 November 2007

Abstract

A prototype Transition Radiation Detector (TRD) with a novel configuration was built and tested. The prototype consists of two individual multiwire proportional chambers (MWPCs) that share a thin common central pad readout electrode. In this way, the TR detection efficiency increases at no penalty in counting speed or in number of readout channels. Measurements with electrons, pions and protons with momentum up to 2 GeV/c show a good position resolution smaller than 200 μm for tracks with normal incidence and no significant deterioration of the resolution is observed up to a particle flux of 200 kHz/cm^2. These results open the possibility of constructing detectors for tracking and e/π discrimination even for high counting rate experiments with a reasonable number of layers. The results on position resolution as well as on rate capability of the prototypes are presented.

PACS: 29.40.Cs

Keywords: Transition radiation detector; Position resolution; Multiwire proportional chamber

1. Introduction

Transition Radiation Detectors (TRDs) are proposed for lepton identification within the CBM (Compressed Baryonic Matter) Experiment [1] at the future FAIR (Facility for Antiproton an Ion Research) [2] facility at GSI (Gesellschaft für Schwerionenforschung). The CBM collaboration proposes to build a dedicated heavy-ion experiment to investigate the properties of highly compressed baryonic matter produced in nucleus-nucleus collisions at FAIR. CBM is designed as a fixed target experiment, in which a TRD will provide tracking of all charged particles, electron identification and discrimination against a large pion background. In conjunction with a RICH detector and an electromagnetic calorimeter the TRD has to provide a sufficient electron identification capability for measurements of charmonium and low-mass vector mesons.

In the TRD transition radiation (TR) is produced in radiators composed of polypropylene foils or, alternatively, *Rohacell* HF71 fibers, only by very fast particles with $\gamma \gtrsim 1000$. At momenta of 1.5 GeV/c only electrons produce TR whereas pions and protons do not [3]. This leads to a significant increase of the signal amplitude measured in the detector with electrons, which is essential for improving electron/pion separation.

For the CBM TRD the required pion suppression is larger than a factor 100 and the required position resolution is of the order of 200−300 μm [4]. In order to fulfill these tasks, in the context of high count rates up to 150 kHz/cm^2 and high particle multiplicities in CBM [5],

*Corresponding author. Tel.: +49 2518334976; fax: +49 2518334962.
E-mail address: kleinboesingme@uni-muenster.de (M. Klein-Bösing).

0168-9002/$ - see front matter
doi:10.1016/j.nima.2007.11.008

simple multiwire proportional chambers (MWPC) based TRDs are obvious candidates for high granularity fast detectors if the gas thickness is reduced to reach the required speed and to reduce space charge effects in a high counting rate environment [6]. However, reducing the detector volume causes a smaller conversion efficiency of the transition radiation in a single layer of the detector. In order to circumvent this aspect, we designed TRD prototypes based on a symmetric arrangement of two MWPCs with a common, central pad readout electrode. These prototypes have already shown a very good discrimination capability of electrons versus pions which meets the requirements of the CBM Experiment [7]. A good efficiency can only be reached with a very thin readout electrode (pad plane) with low absorption between two detector sections. At the same time small pad sizes are needed for a good position resolution. In this paper the results on position resolution as well as on rate capability of the prototypes are presented.

2. Prototype design

A conceptional drawing of the prototype is shown in Fig. 1. The central double-sided pad-structure electrode separates the detector into two identical sections, each of them forming MWPC halves. The two anode planes, placed at either side of the central pad plane, are made of gold plated tungsten wires with a diameter of 20 μm and a wire pitch of 2.5 mm. The double-sided readout electrode has two rows each of them with 9 pads. It is made of a 25 μm kapton foil, on both sides evaporated with a copper pad structure of 0.3 μm thickness. The pad size is $5 \times 10\,\mathrm{mm}^2$ and the corresponding pads on both surfaces are connected. The pad signals are amplified with a 16-channel ASIC preamplifier/shaper with a peaking time of about 70 ns [8] and sampled with a 25 MHz ADC (8 bit, nonlinear).

3. Experimental setup

The in-beam tests were performed in a joint measurement campaign of the JRA4-I3HP collaboration. The common setup is shown in Fig. 2.

The detectors discussed in this paper are the first two of the three detectors labeled M-B (Münster-Bucharest) TRD. The prototypes were tested at different gas gains and beam intensities, different Xe-based gas mixtures (with 10%, 15%, and 20% CO_2 as quencher) and at momenta up to 2 GeV/c for pions, electrons and protons. The beam intensity was varied by changing the extraction time from the SIS accelerator and it was determined by two arrays of four plastic scintillators each (PL1 and PL2).

4. Pulse height distribution

An example of average signals for a momentum of 1.5 GeV/c is shown in Fig. 3.

Due to the slow-moving Xe ions created in the gas avalanche the spectra have long ion tails identifiable in higher time bins. The averaged pulse height is measured at

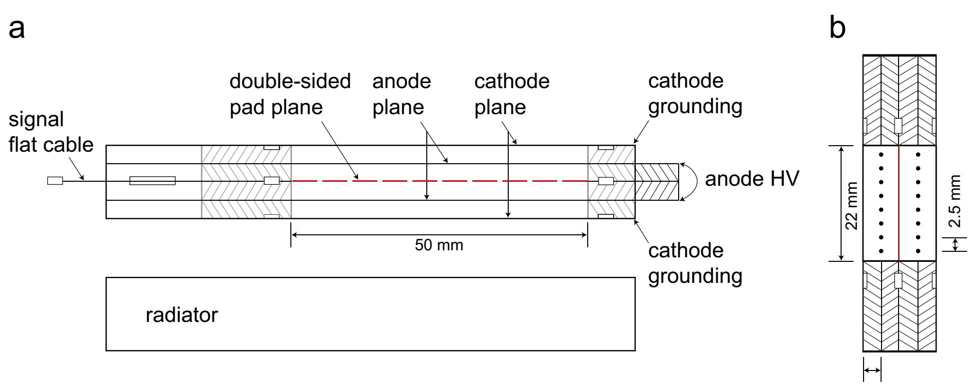

Fig. 1. Schematic configuration of the so-called M-B TRD prototype: (a) projection on a plane perpendicular to the detector surface and parallel to the wire direction and (b) projection on a plane perpendicular to the detector surface and anode wire direction.

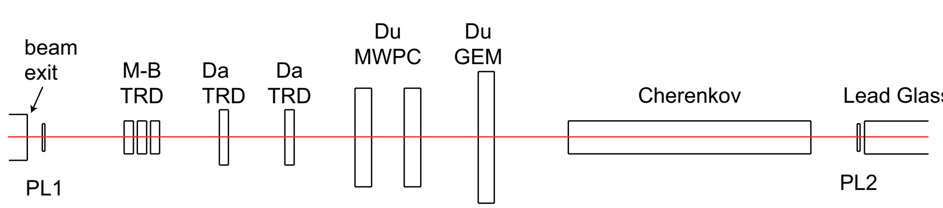

Fig. 2. Experimental configuration used for the in-beam tests. PL1 and PL2 are arrays of plastic scintillator strips for time-of-flight (TOF) and beam rate measurements. A Cherenkov counter and a lead-glass calorimeter are used for electron-pion discrimination. The detectors discussed in this paper are the M-B TRDs. The other prototypes (Da TRD, Du MWPC and Du GEM) are not discussed here.

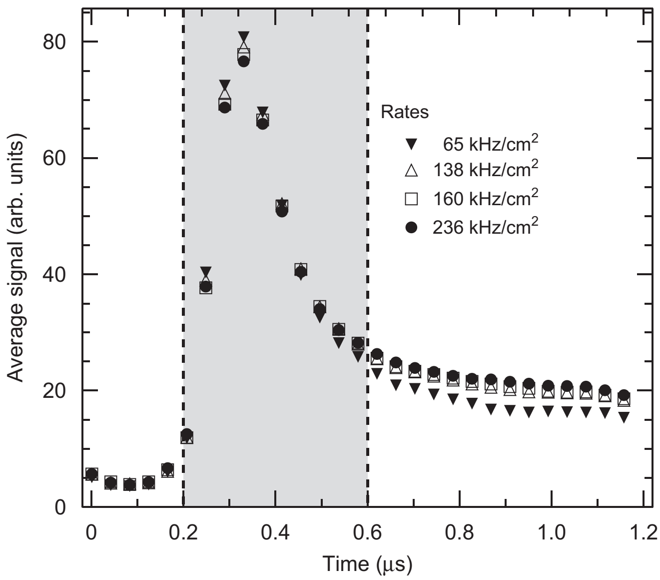

Fig. 3. Average pulse height (charge integral on three adjacent pads) as function of time for different particle rates.

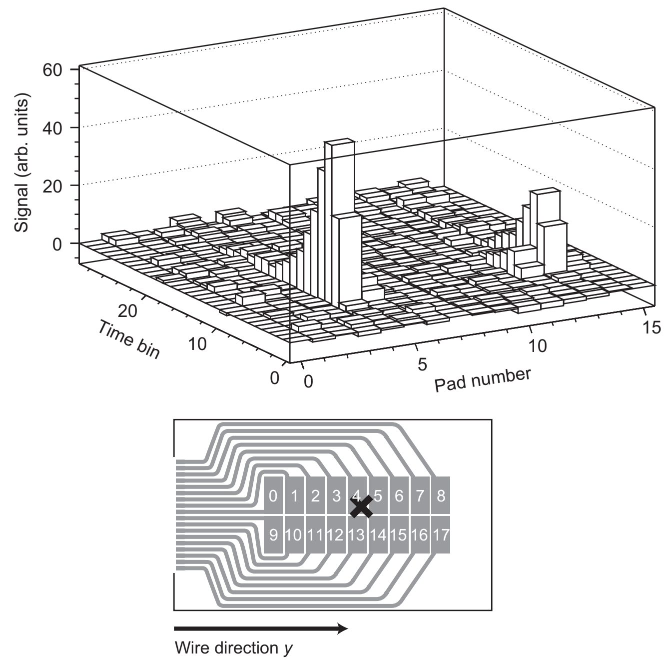

Fig. 4. The upper plot shows the pulse height versus time on 16 readout pads for an example event (16 pads were operated: 0–7 and 8–15). In the lower picture a schematic view of the readout pad structure with the labeled hit position of the same event is shown.

different particle rates: the rate is averaged over the spill length and divided by the full width at half maximum of the beam profile. Only a slight degradation of the amplitude and extension of the ion tails is observed for very high rates up to $240\,\mathrm{kHz/cm^2}$. For the charge integration on the pads the signals in the time interval $0.2-0.6\,\mu\mathrm{s}$ are used, because the avalanche signal is located in this time region (grey band in Fig. 3). The integrated charge in this region shows only a weak dependence on the rate of $<2\%$.

5. Position resolution

5.1. Pad response function

The inner cathode plane of the TRD is subdivided into two rows each consisting of nine separate pads with independent charge sensitive readout (see Fig. 4).

The measurement of the coordinate of the avalanche along the wire direction is done by interpolating the pulse height recorded on adjacent readout pads of width W. The degree of charge sharing is measured by the pad response function (PRF), defined as the ratio of the charge deposited on the central pad to the total charge on all pads as function of the position of the hit relative to the pad center.

The empirical formula by Mathieson [9] for the induced charge distribution $\rho(y)$ describes well the average behavior in symmetric MWPCs along the anode wires, where the y-coordinate is given by the wire direction (see Fig. 4). The PRF is obtained by integration of $\rho(y)$ over the width of the pad with maximum charge

$$P(y) = \int_{y-W/2}^{y+W/2} \rho(y')\,\mathrm{d}y'. \tag{1}$$

In Fig. 5(a) the measured PRF and a comparison to the Mathieson formula is shown. The empirical formula fits very well to the measured PRF which can also be approximated by a Gaussian curve (Fig. 5(b)). The widths σ of Gaussian fits to $P(y)$ are 0.541 ± 0.004 and 0.541 ± 0.003 pad units for the measured PRFs of the two prototypes.

5.2. Cluster reconstruction

Once the variance of the PRF is measured, one can determine the displacement dis_y of the hit from the center of pad i (pad with maximum charge) using pads $i-1$ and i or, alternatively, pads i and $i+1$. The best results are obtained by combining these two measurements of y to a weighted average with weights w_1 and w_2 [10]:

$$\mathrm{dis}_y = \frac{1}{w_1 + w_2}\left[w_1\left(-\frac{W}{2} + \frac{\sigma^2}{W}\cdot\ln\frac{Q_i}{Q_{i-1}}\right) + w_2\left(\frac{W}{2} + \frac{\sigma^2}{W}\cdot\ln\frac{Q_{i+1}}{Q_i}\right)\right]. \tag{2}$$

Here σ is the variance of the Gaussian fitted to PRF and W is the pad width. Since the measurement error is roughly inversely proportional to the recorded pulses on the side pads, one can choose $w_1 = Q_{i-1}^2$ and $w_2 = Q_{i+1}^2$, with Q_i being the charge on pad i. With the knowledge of the displacement the cluster position can be reconstructed.

5.3. Position resolution

For a given track one can define residuals as the distance between the position of the reconstructed y_{cl} and the fitted

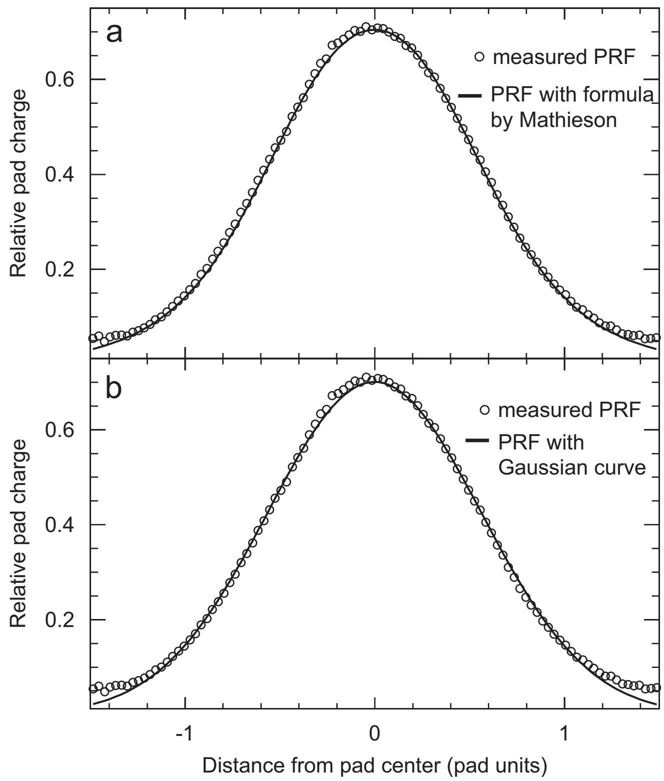

Fig. 5. Pad response functions for $W = 0.5\,\mathrm{cm}$. The circles show the measured PRF. In (a) the line shows the results of a calculation using the Mathieson formula [9] and in (b) the line shows a Gaussian fit to the measured PRF.

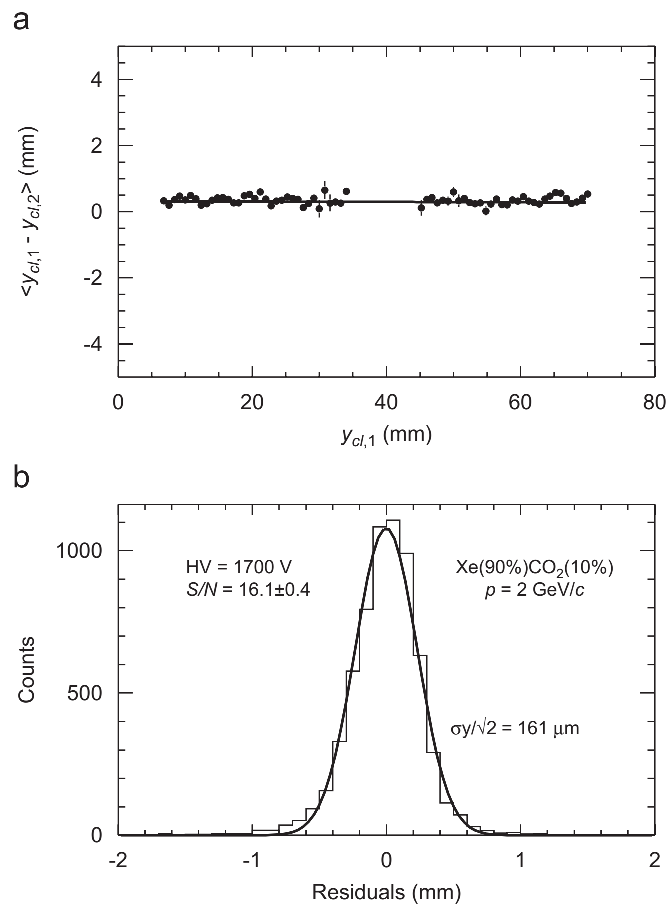

Fig. 6. (a) Linear fit to the alignment of two M-B TRD chambers and (b) distribution of residuals with a Gaussian fit for a single run.

y_{fit} value of the cluster position (see Fig. 6(a)):

$$\Delta_y = y_{\text{cl}} - y_{\text{fit}}. \qquad (3)$$

The position resolution σ_y of two detectors is given by the variance of a Gaussian fitted to the distribution of residuals Δ_y for a large number of tracks. With this method no external tracking devices are needed for the position determination. Since the two prototypes are identical in construction, the position resolution of a single prototype is given by $\sigma_y/\sqrt{2}$. A typical distribution of residuals for moderate particle rates is shown in Fig. 6(b). This resolution of two prototypes does not depend on external effects like multiple scattering in front of the gas volume of the wire chamber and/or beam divergence. It thus represents the intrinsic position resolution of two identical prototypes.

Since the information on both adjacent pads is needed, events with maximum induced charge on a border pad are not considered for the determination of the position resolution. In addition, multiple hits at very high rates are removed by a cut on the charge ratio of the adjacent pads. Fig. 7 shows the rate dependence of the position resolution with a constant efficiency. In all measurements the fraction of the used hits for calculating the position resolution is 25.2%.

We vary the signal to noise ratio S/N and thus the gain by changing the anode voltages. Increasing S/N leads to a better position resolution. The best resolution of $141 \pm 4\,\mu\mathrm{m}$ has been measured at the highest anode voltage of 1850 V ($p = 2\,\mathrm{GeV}/c$ and Xe(80%)CO_2(20%) gas mixture). However, for the measurement of the rate dependence shown in Fig. 7 a moderate voltage of 1700 V has been chosen, to prevent the chambers at high rates from instabilities. In these measurements the most probable

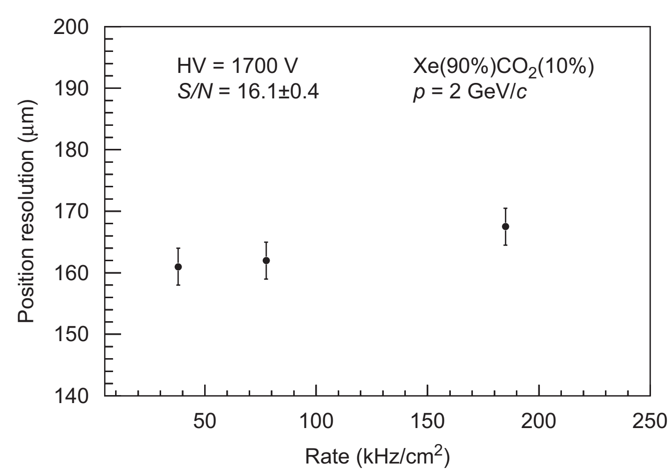

Fig. 7. Position resolution as a function of particle rates with HV = 1700 V and $p = 2\,\mathrm{GeV}/c$, using a Xe(90%)CO_2(10%) gas mixture.

value of the S/N, obtained from a Landau fit to the S/N spectrum, is 16.1 ± 0.4.

For Xe(90%)CO_2(10%) the value of the position resolution at moderate intensity is $161 \pm 3\,\mu m$ or 3.2% of the pad width. No significant deterioration of the position resolution is observed up to average particle rates of $200\,kHz/cm^2$, where it is still better than the desired $200\,\mu m$.

6. Conclusion

The performance of this new type of TRD, based on a double-sided pad readout electrode, has been investigated in terms of counting rate and position resolution. The position resolution is better than $200\,\mu m$ for particle rates up to $200\,kHz/cm^2$ well in line with the design goals of the CBM TRD. The results encourage the further development of this design principle for a TRD in a high counting rate environment.

Acknowledgment

This work was supported by the JRA4-I3HP project (Contract number RII3-CT-2004-506078) financed by EU-FP6.

References

[1] The CBM collaboration, Technical Status Report, February 2005, ⟨http://www.gsi.de/documents/DOC-2005-Feb-447.html⟩.
[2] FAIR Baseline Technical Report, September 2006, ⟨http://www.gsi.de/fair/report/btr.html⟩.
[3] B. Dolgoshein, Nucl. Instr. and Meth. Phys. Res. A 326 (1993) 434.
[4] A. Andronic, Nucl. Instr. and Meth. Phys. Res. A 563 (2006) 349.
[5] V. Friese, Nucl. Phys. A 774 (2006) 377.
[6] M. Petris, et al., Nucl. Instr. Meth. Phys. Res. A 581 (2007) 406.
[7] M. Petrovici, et al., Nucl. Instr. and Meth. Phys. Res. A 579 (2007) 961.
[8] H.K. Soltveit, et al., GSI Scientific Report (2005) 72.
[9] E. Mathieson, Nucl. Instr. and Meth. Phys. Res. A 270 (1988) 602.
[10] W. Blum, L. Rolandi, Particle Detection with Drift Chambers, Springer, Berlin, 1994.